Laser-induced SnO_2 crystallization and fluorescence properties in Eu^{3+}-doped SnO_2-SiO_2 glasses

Masayuki Nogami,* Atsusi Ohno, and Hongpeng You
Nagoya Institute of Technology, Showa Nagoya, 466-8555 Japan
(Received 1 May 2003; published 23 September 2003)

SnO_2 nanoparticles having an average particle size of 5 nm were precipitated in transparent glasses by irradiation with an 800-nm femtosecond laser pulse. Glasses, prepared to codope Sn^{4+} and Eu^{3+} ions by a sol-gel method, were heated in a H_2 gas atmosphere, in which the Sn ions are coordinated by two oxygen ions with point defect of a molecularlike electronic structure. Upon laser pulse irradiation, the twofold-coordinated Sn atoms are activated to react with oxygen, resulting in the formation of SnO_2 nanocrystals. The precipitated SnO_2 crystals grew up to circa 5-nm size by the Joule-heating effect of the laser. The fluorescence intensities of the codoped Eu^{3+} ions were enhanced higher than 100 times that of the glass without nanocrystals by exciting with an energy corresponding to the absorption edge of the SnO_2 nanocrystals, the energy of which is effectively transferred to the Eu^{3+} ions. It was found that the Eu^{3+} ions are located in the glass structure from the fluorescence line narrowing spectroscopy.

DOI: 10.1103/PhysRevB.68.104204 PACS number(s): 78.55.Qr, 78.67.Bf, 81.16.Mk

I. INTRODUCTION

The local modification of the optical properties of transparent glasses has become very important because of its high potential use in photonic applications such as amplifiers, fibers, filters, memories, and so forth.[1–4] The primary object of this strategy involves the fabrication of glasses with one-, two-, or three-dimensionally local modified structures. One way to obtain this modification is to use high power beams such as electrons, x rays, and lasers that are capable of inducing a local structural modification in glasses. Komatsu's group used a continuous-wave yttrium aluminum garnet laser to precipitate optical nonlinear crystals.[5–7] Visible or violet lasers have also been applied for the spatially selected crystallization in glasses.[8,9] The crystallization process is considered to take place due to the thermal effect of the laser irradiation. Recently, Hirao and Qiu's group used an infrared femtosecond pulsed laser for the formation of photoinduced refractive-index spots in glasses.[10] They also reported the space-selective photoreduction of rare-earth ions in glasses using an infrared femtosecond laser.[11–13] They considered that the active electrons and holes created by the multiphoton ionization, Joule heating, and collisional ionization caused reduction of the rare-earth ions.

We also used x rays or lasers to reduce the Sm^{3+} ions to Sm^{2+} in glasses. The photoreduced Sm^{2+} ions exhibited very fast hole-burning formation with deep holes compared to that of the Sm^{2+} ions reduced by a H_2 gas treatment.[14,15] Thus, the laser pulse becomes a technique for producing photonic glasses. More recently, we succeeded in precipitating nanosized SnO_2 crystals by irradiating the femtosecond laser into sol-gel-derived glasses containing Sn and Eu ions, and observed very strong fluorescence intensities of the Eu^{3+} ions from the laser-irradiated spots. These changes in properties can be space-selectively controlled in glasses by changing the position of the laser irradiation, and these glasses provide a bright prospect for their optical applications. However, the question as to how the laser irradiation affects the precipitation of the SnO_2 crystals and the fluorescence properties of the rare-earth ions still remains unknown.

The aim of this work is to study the growth dynamics of the SnO_2 crystals by the laser irradiation and fluorescence properties of the Eu^{3+} ions. The femtosecond laser pulse was irradiated in the sol-gel-derived glasses under various conditions to precipitate the nanosized SnO_2 crystals. The enhanced fluorescence of the Eu^{3+} ions is discussed related to the size effect of the SnO_2 crystals. The local structure around the Eu^{3+} ions is also studied using the fluorescence line-narrowing spectra. This report is very significant when considering the reaction of glass under laser irradiation and the application of a femtosecond laser to glass modification.

II. EXPERIMENT

A. Sample preparation

Using the sol-gel method, $5SnO_2 \cdot 95SiO_2$ (mol %) glasses were prepared and contained 1-wt % Eu_2O_3. The materials, $EuCl_3 \cdot 6H_2O$, $SnCl_2 \cdot 2H_2O$, and $Si(OC_2H_5)_4$, are commercially available, and were used as received. $Si(OC_2H_5)_4$ was first hydrolyzed at room temperature with a mixed solution of H_2O, C_2H_5OH, and HCl. Separately, $SnCl_2 \cdot 2H_2O$ dissolved in C_2H_5OH was added to the starting solution. After stirring for 0.5 h, $EuCl_3 \cdot 6H_2O$ dissolved in C_2H_5OH was added to this solution with stirring. The resultant homogeneous solution was hydrolyzed by adding the mixed solution of H_2O, C_2H_5OH, and HCl, followed by storage at room temperature for about two weeks to form a stiff 1–3-mm-thick gel. The quantities of the chemistries used in this experiment were described elsewhere.[16] To completely hydrolyze the alkoxide, the gel was heated in a sealed vessel together with water at 150 °C for 30 h, followed by heating in air at 700 °C for 5 h. The prepared glasses were further heated at temperatures above 500 °C under a flowing mixed gas with 20% H_2-80% N_2 for 5 h.

B. Laser irradiation and characterization

The laser irradiation was performed using a Ti:sapphire laser operating at 800 nm with a 1-kHz repetition rate and a 130-fs pulse (Spectra-Physics, Hurricane) at room tempera-

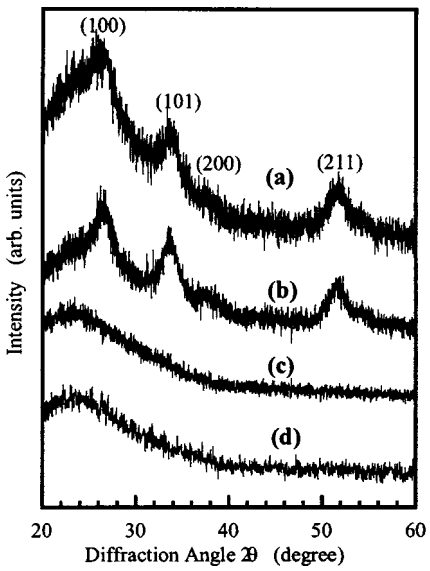

FIG. 1. X-ray diffraction patterns of Eu^{3+} ion-doped $5SnO_2 \cdot 95SiO_2$ glass heated in air at 500 °C (curve a), and 700 °C (curve b), followed by heating in H_2 gas at 500 °C (curve c), and 600 °C (curve d). Numbers are indexed as a tetragonal SnO_2 crystal.

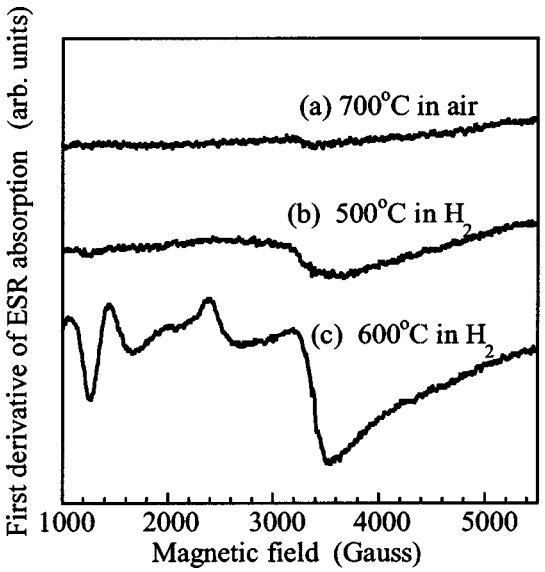

FIG. 2. Electron spin resonance spectra of Eu^{3+} ion-doped $5SnO_2 \cdot 95SiO_2$ glass heated at 700 °C in air (curve a), followed by heating in H_2 gas at 500 °C (curve b), and 600 °C (curve c).

ture. A laser beam with an average power of 720 mW was focused by an objective lens with the spot size of ~0.4 mm in diameter into the interior of the glass. The laser power was lower than for the damage threshold of glass, but a faint coloration of the exposed region was observed.

The crystalline data were gathered using x-ray diffractometry (XRD; Rigaku RAD-B system Cu $K\alpha$; 40 kV, 20 mA) and transmission electron microscopy (TEM; JEOL JEM-100C 100 kV). For the fluorescence (FL) measurement, a N_2 laser (Laser Photonics wavelength; 337.1 nm, pulse width; <1 ns) was used as an excitation source. The FL intensity in each of the pulsed illuminations was monitored at a right angle by a silicon photo-diode and an oscilloscope. The gate width was changed to the lifetime of the FL intensity. The electron spin resonance (ESR; JASCO, JES-FE ME3X) measurement was performed at room temperature. The g values of the measured signals were calibrated by the utilization of diphenyl-picrylhydrazal. The fluorescence line-narrowing spectra (FLN) measurement of the Eu^{3+} ions was performed under excitation with a wavelength within the $^7F_0 \rightarrow {}^5D_0$ transition by a rhodamine 6G dye laser. The FL intensity was measured with a chopper that alternately opened the optical paths before and after the sample. All spectra were recorded at 7 K.

III. RESULTS AND DISCUSSION

A. Status of Sn ions in sol-gel-derived glasses

Both the glasses heated in air and H_2 atmospheres appeared transparent and colorless, while enormous difference was observed in their structures. Figure 1 shows typical XRD patterns of the glasses obtained by heating under various conditions. The diffraction peaks that appeared in the samples heated in air at 500 °C and above (curves *a* and *b*) are assigned to the (100), (101), (200), and (211) planes of the tetragonal rutile-type SnO_2 crystals, indicating the precipitation of SnO_2 crystals. The crystal size was calculated from the magnitude of the line broadening using Scherrer's equation; 6.6 and 8.5 nm for glasses heated at 500 and 700 °C, respectively. TEM observations also confirmed the presence of the SnO_2 particles with a size of 6–10 nm without agglomeration of the particles.

In the glasses heated in a H_2 atmosphere, on the other hand, there was a drastic change in the XRD spectra. The XRD peaks corresponding to the SnO_2 crystals completely vanished, as shown in curves *c* and *d* of Fig. 1. The redox equilibrium of stannic oxide in oxygen and hydrogen gas atmospheres is determined by the affinity of tin and hydrogen to oxygen. The affinity of the cation to oxygen is estimated from the standard free energy of formation of the oxides. The cation of which the affinity is small is reduced. Compared with the free energy of the H_2O formation, the SnO_2 has high a free energy and is easily reduced into SnO and Sn in the reduced atmosphere. Thus, annealing in the H_2 atmosphere above 232 °C (melting point of Sn metal) causes the decomposition of the SnO_2 crystals into Sn and the dissolution in the SiO_2 glass matrix.

The heating temperature in H_2 gas is important for obtaining the transparent, colorless glasses. The sample heated above 600 °C became slightly gray in color, while the glass heated at 500 °C was colorless. Shown in Fig. 2 are the ESR spectra of the same samples. A small and broad signal is observed around 3300 mT in both spectra for the glasses heated in air (a) and H_2 gas at 500 °C (b), which can be assigned to the hole centers from the comparison of the g value with that of the free electron. The glass heated in H_2 gas at 600 °C, however, exhibits the strong ESR signals between 1200 and 2500 mT, which are attributed to the Eu^{2+} ions. The Eu^{2+} ions give a strong optical absorption around 400 to 550 nm in wavelength. Thus, the heating in H_2 gas below 600 °C was needed to obtain the transparent glasses.

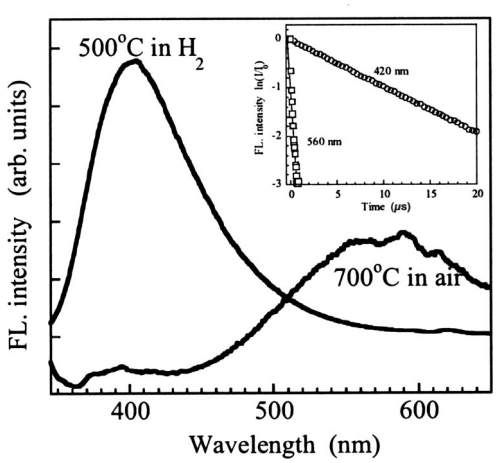

FIG. 3. Fluorescence spectrum of glasses heated at 700 °C in air, followed by heating in H_2 gas at 500 °C. The inset shows the fluorescence decay curve of the 420- and 560-nm bands.

The status of the Sn and Eu ions in glasses was also examined from the measurements of the FL spectra at room temperature. For the glass heated in air at 700 °C, in addition to the FL spectra of the Eu^{3+} ions with the lifetime of the ms order, a broadband FL spectrum was observed around 560 nm by photoexciting at around 330 nm. This spectrum is shown in Fig. 3. The lifetime was estimated to be 0.5 μs from the decay curve of the FL intensity (see the inset of Fig. 3). It is well known that oxygen-deficient sites in SnO_2 crystals are easily formed, which emit a broad luminescence in the visible region with a short lifetime. The apparent similarities of these FL properties strongly suggest the existence of the oxygen-defect sites in the SnO_2 crystals precipitated in the present glass.

After the H_2 annealing, the FL intensity around 560 nm disappeared, while a substitutionally strong FL band peaking at 420 nm was observed, as shown in Fig. 3. Two possible origins for this FL can be considered: the existence of Eu^{2+} ions and Sn-related defects. No ESR signal for the Eu^{2+} ions around 1200 mT was detected (see Fig. 2), indicating that the Eu^{3+} ions stably remain in glass heated at 500 °C in a H_2 atmosphere. The lifetime of this fluorescence was estimated as 10 μs (see the inset of Fig. 3). Furthermore, the excitation spectrum of the 420-nm FL was measured to have three bands at 190, 265, and 355 nm.[17] These energies reflect the molecularlike energy structure of the excited state of the singlets (S_2, S_1) and triplet (T_1) singlet ground state (S_0), respectively, which is in excellent agreement with the previous observations by Skuja[18] and Chiodini[19] who reported the FL properties of the Sn-doped glasses. Based on these ESR and fluorescence properties, the 420-nm FL can be assigned to defects with a molecularlike electronic structure in the twofold-coordinated Sn atoms, named the Sn_2^0 centers. Thus, we can conclude that there exist twofold-coordinated Sn atoms and Eu^{3+} ions in the glass heated in H_2 at 500 °C.

B. Precipitation of SnO_2 nanocrystals by laser irradiation

A Ti:sapphire laser with a 1-kHz repetition rate and a 130-fs pulse duration was irradiated into the glass heated in H_2 gas at 500 °C. A TEM photograph of the laser irradiated position is shown in Fig. 4. It is evident that the particles having an average particle size of circa 5 nm are clearly observed, which are assigned to SnO_2 crystals based on the electron diffraction analysis.

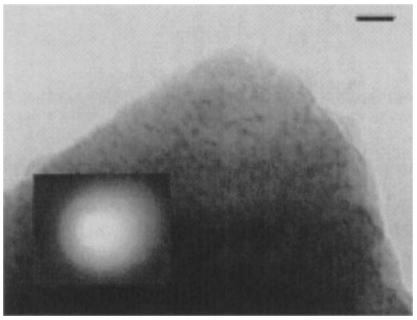

FIG. 4. Transmission electron microscopic photograph of the laser irradiated glass. The bar scale is 20 nm. The inset shows the electron diffraction pattern.

When irradiated with a laser, we observed the emission of an instant but strong white light from the laser-focused area. It has been reported that a white light supercontinuum is observed below the threshold of the laser-induced damage.[20–22] Figure 5 shows the time-resolved spectra of the white light within the first few seconds of the laser irradiation. Note that the broad fluorescence band peaking around 450 nm is caused by the laser irradiation, the intensity of which drastically decreases during irradiation. The dependence of the FL intensities on the laser irradiation period is shown in Fig. 6 as a function of the laser irradiation time. It is evident that the white light emission is completed within a few seconds of laser irradiation. We confirmed that this whitelight is emitted neither from the sample irradiated in a vacuum, nor the sintered-nonporous glasses. No SnO_2 crystal precipitation was observed in these glasses. It was also observed that the 420-nm FL band, which is observed for the sample heated in H_2 gas and assigned to the Sn_2^0 centers, disappears after laser irradiating for 5 sec or more. These experimental results clearly indicate that oxygen in air plays

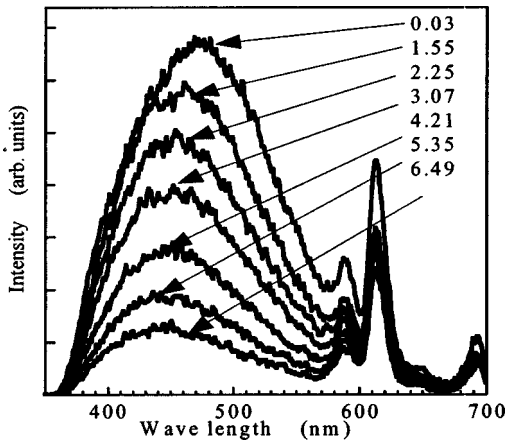

FIG. 5. Time-resolved emission spectra of glass during irradiation with a femtosecond laser pulse. Numbers are laser irradiation period in seconds.

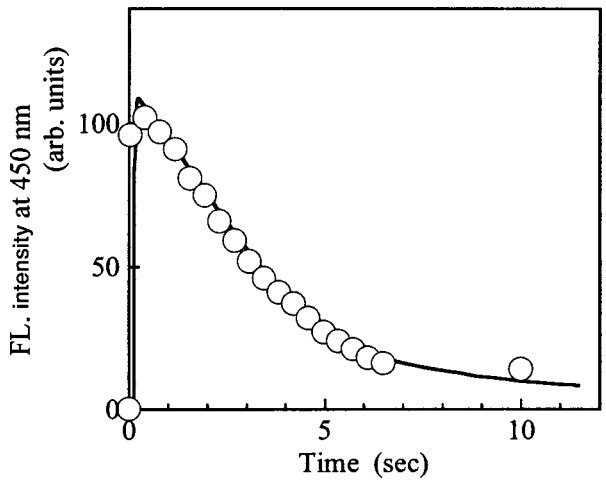

FIG. 6. Dependence of the emission intensity at around 450 nm on the laser irradiation period.

an important role in the formation of the SnO_2 crystals. We can consider the formation of SnO_2 crystals by the photoactivation/ionization of the twofold-coordinated Sn_2^0 centers and reaction with oxygen molecules. Lone pair electrons in the Sn_2^0 centers are sensitive to ionizing into the activated state, resulting in a reaction with oxygen ions, thus forming SnO_2;

$$Sn_2^0 + O_2 = SnO_2 .$$

Our glasses, prepared by the sol-gel method, are porous. These pores, which permit the oxygen to diffuse quickly through the pores, result in the easy reaction between the glass constituent ions and oxygens. Thus the sol-gel-derived glasses easily undergo modification of their microstructures.

Prolonged laser irradiation causes the fluorescence band around 560 nm, as shown in Fig. 7. The properties, the position and the lifetime, of this fluorescence are the same as those shown in Fig. 3, indicating that the oxygen defect centers are formed in the precipitated-SnO_2 crystals. In the inset of Fig. 7, the fluorescence intensities of the 560-nm FL band are plotted as a function of the laser irradiation time, where the intensities are normalized to a saturated value after prolonged irradiation. It is evident that the FL intensity increases with the increasing laser irradiation time after the threshold time of about 100 sec. The increased FL intensity can be considered to be related to the growth of the SnO_2 crystals, so that the FL intensities correspond to the amount of SnO_2 crystals precipitated in the glass. The dynamics of crystal growth was examined using an Avramid type equation for the data in Fig. 7:

$$F = 1 - \exp\{-K(t - t_0)\},$$

where F is the volume fraction of a crystal at time t, and K and t_0 are the rate constant and the threshold time for the crystal growth, respectively. A good fitting was obtained for the value of $K = 0.0012$/sec, indicating that the prolonged laser irradiation causes the Joule-heating effect of the exposed area, resulting in crystal growth. Our laser irradiation method in the sol-gel-derived glasses has an advantage over the heating process of glass because of the possibility of space-selective precipitation by moving the focused point of the laser.

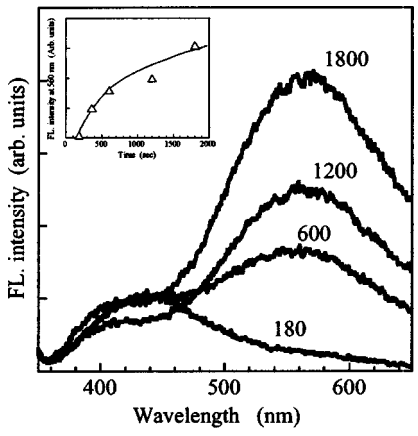

FIG. 7. Fluorescence spectra, excited at a 337-nm N_2 laser, of glasses irradiated with a laser pulse. The gate width was 0.1 μs. Numbers are laser irradiation periods in seconds. The inset shows the dependence of the emission intensity at 560 nm on the laser irradiation period.

C. Fluorescence properties of Eu^{3+} ions affected by crystal growth of SnO_2

Our glasses have been prepared to contain the Eu^{3+} ions. Before the laser irradiation, the FL intensity was very low (see Figs. 3 and 8) and compared with those observed in the SiO_2 glass containing the Eu^{3+} ions. It is known that the FL properties of rare-earth ions are strongly influenced by the matrix structure. We reported the Eu^{3+} ion aggregation in the SiO_2 glass matrix, where an energy transfer between Eu^{3+} ions causes a quenching of the FL efficiency.[23] The addition of a third component such as Al_2O_3 is quite effective for the elimination of the Eu^{3+} aggregation due to the formation of a negatively charged AlO_4^- tetrahedral, which results in the increased FL intensities.[23,24] For a SnO_2-SiO_2 glass prepared by the sol-gel process, however, the twofold-coordinated Sn_2^0 centers do not act to disperse the Eu^{3+} ions in the network structure, which weakens the FL intensity.

We found that after laser irradiation, the FL intensity of the Eu^{3+} ions is strongly increased. Figure 8 shows the FL spectra of the laser-irradiated glass for different irradiation periods. The excitation for the fluorescence measurement used a N_2 laser of 337.1-nm wavelength. The FL bands peaking around 600 nm are assigned to the $^5D_0 \rightarrow {}^7F_{j\ (j=0,1,2,3)}$ transitions of the Eu^{3+} ions. It is evident that the FL intensity of the Eu^{3+} ions increases with the increasing irradiation period, reaching an intensity greater than 100 times that of the glass before laser irradiation. The spot of the red emission developed until it was visible to the naked eye. No fluorescence of the Eu^{2+} ions was observed after laser irradiation, suggesting that the Eu^{3+} ions are stable in the glass against laser irradiation. The fluorescence intensities of the

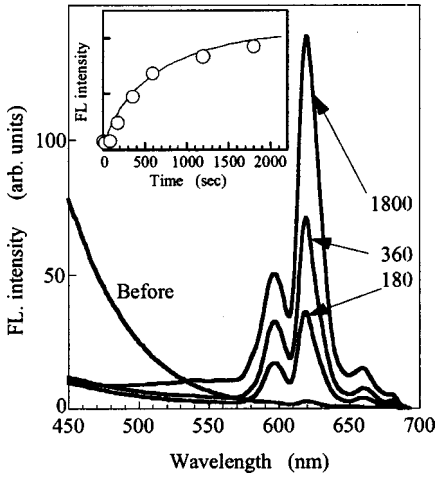

FIG. 8. Fluorescence spectra, excited at a 337-nm N_2 laser, of glasses before and after laser irradiation. Numbers are laser irradiation periods in seconds. The inset shows the dependence of the emission intensity at 620 nm on the laser irradiation period.

Eu^{3+} ions are plotted in the inset of Fig. 8 as a function of the laser irradiation period. The FL intensities increase with increasing time and approach a saturated level. It is interesting to note that its time dependence of the FL intensity resembles that for that of the FL at 560 nm (Fig. 7), suggesting that the crystal growth of the SnO_2 affects the fluorescence properties of the Eu^{3+} ions. There are two channels of excitations in the Eu^{3+} fluorescence: direct excitation of the Eu^{3+} ions in the glass network and indirect excitation from the SnO_2 nanocrystals into the Eu^{3+} ions. Figure 9 shows the excitation spectra, monitored by the fluorescence of the $^5D_0 \rightarrow {}^7F_2$ transition at 620 nm, for glasses before and after the laser irradiation. All the sharp lines, observed at wavelengths from 465 to 350 nm are assigned to the *f-f* transitions within the Eu^{3+} ions. It is apparent that the intensities of the direct *f-f* transitions within the Eu^{3+} ions are gradually increased by the laser irradiation, indicating that the concentration quenching of the FL intensities is effectively released by the crystallization. In addition to these lines, a broad and

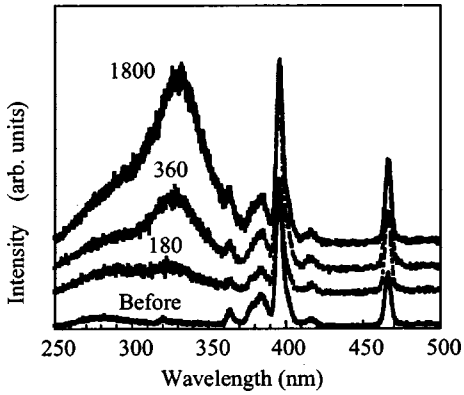

FIG. 9. Fluorescence excitation spectra, monitored by the fluorescence of the $^5D_0 \rightarrow {}^7F_1$ transition at 620 nm of the glass before and after laser irradiation. A xenon lamp was used for the excitation.

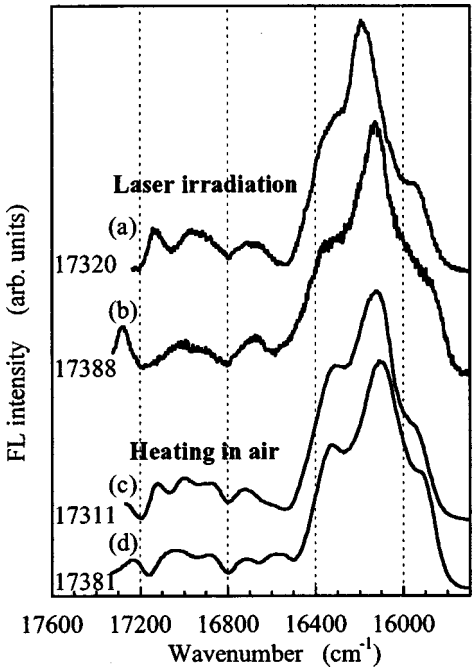

FIG. 10. Fluorescence line narrowing spectra of the Eu^{3+} ion-doped glasses prepared by laser irradiation (curves a and b) and heat treatment in air at 700 °C (curves c and d). The numbers indicate the wave number of the excitation laser beam.

strong band is observed from 280 to 350 nm only in the laser-irradiated glass, the intensity of which increases with the increasing laser irradiation period. This excitation energy coincides with the absorption edge energy of the SnO_2 nanocrystal at ~360 nm. From these experimental results, the following mechanism for the enhanced fluorescence is considered. The electron-hole pairs are generated by the energy absorbed in the nanocrystals, the energies of which are recombined and then transferred into the Eu^{3+} ions, resulting in the enhanced fluorescence. Thus, the existence of the excitation band corresponding to the band gap energy is evidence of the energy transfer from the nano-sized SnO_2 crystal to the Eu^{3+} ions.

Next we consider the environmental structure surrounding the Eu^{3+} ions. The FL spectral feature of the Eu^{3+} ions is strongly reflected by the local environment of the Eu^{3+} ions. The $^5D_0 \rightarrow {}^7F_2$ band at 620 nm is electric dipole transition sensitive to chemical bonds in the vicinity of the Eu^{3+} ion, while the $^5D_0 \rightarrow {}^7F_1$ transition band at 595 nm is a magnetic dipole one and hardly varies with the crystal field strength around the Eu^{3+} ion. Therefore, the fluorescence intensity ratio of the $^5D_0 \rightarrow {}^7F_2$ to $^5D_0 \rightarrow {}^7F_1$ transitions provides a measure of the degree of distortion from the inversion symmetry of the local environment of the Eu^{3+} ion in the matrix. The intensity ratio of the glass after laser irradiation is calculated to be 2.87, which is no different from that for a glass before irradiation, suggesting that the Eu^{3+} ions are embedded in the glass-network structure.

The local environment around the Eu^{3+} ions has been widely studied by the laser induced-FLN spectroscopy. Figure 10 shows the FLN spectra, measured at 7 K after excitation at different energies inside the $^7F_0 \rightarrow {}^5D_0$ transition, of

the Eu^{3+} ions in the laser irradiated-area, where the FLN spectra for glass heated in air at 700 °C are illustrated for comparison. Two groups of FLN bands were observed in the energy ranges of 17 400–16 500 and 16 400–15 800 cm^{-1}, which are assigned to the $^5D_0 \rightarrow {}^7F_1$ and $^5D_0 \rightarrow {}^7F_2$ transitions, respectively. In the spectra (curves *a* and *b*) for the laser-irradiated glass, the $^5D_0 \rightarrow {}^7F_1$ bands appears to consist of three peaks due to Stark splitting of the $^7F_1$ state, indicating that the Eu^{3+} ions are located in a site with C_{2v}, C_2, or C_s symmetry.[25] Of the three $^7F_1$ lines, the highest-energy line, 17 125 cm^{-1} for the 17 320-cm^{-1} excitation, shifts to the higher-energy side with the increasing excitation energy, while the two low-energy lines peaking at 16 960 and 16 695 cm^{-1} become very broad and their positions have a smaller dependence on the excitation energy. We found that this dependence of the peak positions on the excitation energy is not changed from that observed for the glass before laser irradiation. It is also confirmed that the behavior of the three $^5D_0 \rightarrow {}^7F_1$ lines is similar to that reported for the Eu^{3+} ion-doped silicate, borate, phosphate, and fluoride glasses.[26–30] These experimental results strongly suggest that the Eu^{3+} ions are located in the amorphous glass structure. This becomes further clarified from the comparison with the FLN spectra (curves *c* and *d*) for the glass heated in air at 700 °C, where the SnO_2 nanocrystals are precipitated. It is apparent that the $^5D_0 \rightarrow {}^7F_1$ bands are resolved into five lines, e.g., 17 210, 17 021, and 16 720 cm^{-1}, and 16 860, and 16 090 cm^{-1} for the 17381 cm^{-1} excitation (see curve *d*). It is well known that the Sn^{4+} ions in the SnO_2 crystal have a D_{4h} symmetry. If the Eu^{3+} ions occupy the sites of Sn^{4+} ions in the SnO_2 crystal, the Eu^{3+} ions should have the same symmetry to that of the Sn^{4+} ions. According to crystal field theory, the ions at a site with D_{4h} should have two $^5D_0 \rightarrow {}^7F_1$ bands. Compared to the FLN spectra of these glasses, we can attribute the bands peaking at 16 860 and 16090 cm^{-1} to the Eu^{3+} ions located in the SnO_2 crystal. The crystal-symmetrical study of the Eu^{3+} ions will be further discussed elsewhere.

IV. CONCLUSIONS

In this study, we demonstrated that SnO_2 nanoparticles having an average particle size of 5 nm were precipitated in glasses by irradiation with an 800-nm femtosecond laser pulse. The laser irradiation brings about the activated twofold-coordinated Sn atoms and the reaction with oxygen, resulting in the formation of SnO_2 nanocrystals. The precipitated SnO_2 crystals grew to a circa 5-nm size by the Joule-heating effect of the laser irradiation. It was observed that the fluorescence intensities of the codoped Eu^{3+} ions were enhanced greater than 100 times that of the glass without nanocrystals by the energy transfer from the nanocrystals to the Eu^{3+} ions. These glasses can provide a bright prospect for their optical applications such as high-density memory devices.

ACKNOWLEDGMENTS

We thank N. Tanaka of Nagoya University for the TEM observation. This research was partly supported by a Grant-in-Aid for Scientific Research (No. 13305048) from the Ministry of Education, Science, and Culture of Japan and a grant from the NITECH 21st Century COE Program ''World Ceramics Center for Environmental Harmony.''

*Email address: nogami@mse.nitech.ac.jp

[1] O. M. Efimov, L. B. Glebov, S. Grantham, and M. Richardson, J. Non-Cryst. Solids **253**, 58 (1999).
[2] M. Kaempfe, H. Hofmeister, S. Hopfe, G. Seifert, and H. Graener, J. Phys. Chem. B **104**, 11 847 (2000).
[3] M. Watanabe, S. Juodkazis, H. B. Sun, S. Matsuo, and H. Misawa, Appl. Phys. Lett. **77**, 13 (2000).
[4] H. B. Sun, S. Juodkazis, M. Watanabe, S. Matsuo, and H. Misawa, J. Phys. Chem. B **104**, 3450 (2000).
[5] R. Sato, Y. Benino, T. Fujiwara, and T. Komatsu, J. Non-Cryst. Solids **289**, 228 (2001).
[6] T. Honma, Y. Benino, T. Fujiwara, T. Sato, and T. Komatsu, Opt. Mater. (Amsterdam, Neth.) **20**, 27 (2002).
[7] T. Honma, Y. Benino, T. Fujiwara, T. Sato, and T. Komatsu, J. Ceram. Soc. Jpn. **110**, 398 (2002).
[8] T. Honma, Y. Benino, T. Fujiwara, T. Komatsu, and R. Sato, Appl. Phys. Lett. **82**, 892 (2003).
[9] M. A. Camacho-Lopez, S. Vargas, R. Arroyo, E. Haro-Poniatowski, and R. Rodriguez, Opt. Mater. (Amsterdam, Neth.) **20**, 43 (2002).
[10] J. Qiu, K. Miura, and K. Hirao, Jpn. J. Appl. Phys. **37**, 2263 (1998).
[11] J. Qiu, K. Miura, T. Suzuki, and K. Hirao, Appl. Phys. Lett. **74**, 10 (1999).
[12] K. Miura, J. Qiu, T. Mitsuyu, and K. Hirao, Proc. SPIE **3618**, 141 (1999).
[13] K. Miura, J. Qiu, S. Fujiwara, S. Sakaguchi, and K. Hirao, Appl. Phys. Lett. **80**, 2263 (2002).
[14] M. Nogami and K. Suzuki, J. Phys. Chem. B **106**, 5359 (2002).
[15] M. Nogami and K. Suzuki, Adv. Mater. (Weinheim, Ger.) **14**, 929 (2002).
[16] M. Nogami, T. Enomoto, and T. Hayakawa, J. Lumin. **97**, 147 (2002).
[17] T. Hayakawa, T. Enomoto, and M. Nogami, J. Mater. Res. **17**, 1305 (2002).
[18] L. Skuja, J. Non-Cryst. Solids **149**, 77 (1992).
[19] N. Chiodini, M. Meinardi, F. Morazzoni, A. Paleari, R. Scotti, and D. Di. Martino, J. Non-Cryst. Solids **261**, 1 (2000).
[20] A. Brodeur and S. L. Chin, Phys. Rev. Lett. **80**, 4406 (1998).
[21] O. M. Efimov, K. Gabel, S. V. Garnov, L. B. Glebov, S. Grantham, M. Richardson, and M. J. Soileau, J. Opt. Soc. Am. B **15**, 193 (1998).
[22] S. L. Chin, S. Petit, F. Borne, and K. Miyazaki, Jpn. J. Appl. Phys. **38**, L126 (1999).
[23] T. Hayakawa and M. Nogami, J. Appl. Phys. **90**, 2200 (2001).
[24] K. Arai, H. Namikawa, K. Kumata, T. Honda, Y. Ishii, and T. Handa, J. Appl. Phys. **59**, 3430 (1986).

[25] C. Brecher and L. A. Riseberg, Phys. Rev. B **13**, 81 (1976).
[26] M. Tanaka, G. Nishimura, and T. Kushida, Phys. Rev. B **49**, 16 917 (1994).
[27] J. A. Capobianco, P. P. Proulx, M. Bettinnelli, and F. Negrosolo, Phys. Rev. B **42**, 5936 (1990).
[28] T. F. Belliveau and D. J. Simkin, J. Non-Cryst. Solids **110**, 127 (1989).
[29] M. J. Lochhead and K. L. Bray, Chem. Mater. **7**, 572 (1995).
[30] V. C. Costa, M. J. Lochhead, and K. L. Bray, Chem. Mater. **8**, 783 (1996).